telecom

MDPI

Article

A Minimum SER Design for a NOMA-Assisted Pinching-Antenna System

Brian Yshmael Dimaunahan Rito

Independent Researcher, Singapore, Singapore; rito0002@e.ntu.edu.sg

Abstract

By adjusting antenna parameters, flexible antenna systems can dynamically reconfigure wireless channel characteristics to improve system performance. Non-orthogonal multiple access (NOMA) is a promising multiple access technique for enhancing the spectral efficiency and connectivity of next-generation wireless systems. A key research focus is how to leverage the synergy between NOMA and flexible antenna systems. A novel type of flexible antenna system called pinching-antenna system can provide line-of-sight (LoS) links to users by adjusting the position of the pinching antenna, mitigating large-scale fading. In this paper, we investigate how to implement reliable communication in a downlink NOMA-assisted pinching-antenna system by minimizing the symbol error rate (SER). We derive the SER expressions for NOMA-assisted pinching-antenna system users with QAM modulation, and minimize it with respect to the power allocation factor and the position of the pinching antenna. At higher-order modulation, it is revealed that the minimum SER strategy is for the pinching antenna to track the strong NOMA user. Finally, the analysis is verified by Monte Carlo simulation.

Keywords: non-orthogonal multiple access; pinching-antenna system; symbol error rate

1. Introduction

By being able to dynamically adjust the antenna parameters, flexible antenna systems [1] can enhance signal or mitigate interference, thereby improving system performance. Flexible antenna systems have garnered significant research interest and several types have been conceptualized and prototyped. For instance, movable antennas [2] can improve the wireless communication performance by adjusting their position and orientation in the three-dimensional space. Also, fluid antennas [3] can use liquid as radiating elements, which can be configured into many different positions, orientations or shapes inside a fluid container. However, since the movement of the aforementioned flexible antennas is only at the wavelength scale, they cannot be adjusted to primarily compensate for large-scale fading.

A novel type of flexible antenna system called pinching-antenna system [4] can overcome this limitation by being able to provide users with line-of-sight (LoS) links, while at the same time being situated in the users' vicinity, thereby mitigating large-scale fading. Pinching-antenna systems consist of dielectric waveguides and radiation points activated by small dielectric particles, such as plastic pinches, in the waveguide. As the propagation loss in the waveguide is much lower compared to that in free space, activating radiation points with LoS links near the users can mitigate large-scale fading.

To support the massive connectivity and bandwidth demands of the next-generation wireless network, many innovative multiple access techniques, such as orthogonal time

Check for updates

Received: 6 July 2026
Revised: 17 September 2026
Accepted: 28 September 2026
Published: 1 October 2026

Copyright: © 2026 by the author. Licensee MDPI, Basel, Switzerland. This article is an open access article distributed under the terms and conditions of the Creative Commons Attribution (CC BY) license.

frequency space (OTFS)-based multiple access [5], collision-resilient unsourced random access for massive multiple-input multiple-output (MIMO) [6] and non-orthogonal multiple access (NOMA) [7] have been proposed. NOMA is a promising multiple access scheme for enhancing the spectral efficiency and connectivity of future wireless communication systems, offering significant performance improvements over the traditional orthogonal multiple access (OMA) schemes by enabling multiple users to share the same time and frequency resources. A variant of NOMA called power-domain (PD) NOMA implements efficient resource sharing through multiplexing signals with differing power levels and using successive interference cancellation (SIC) at the receiver to sequentially detect superimposed signals. NOMA is expected to be considered as a multiple access scheme candidate for the future 6G network [8]. The beneficial collaboration between the pinching-antenna system and NOMA has recently attracted considerable research focus, and in this article we investigate the reliability of a NOMA-assisted pinching-antenna system.

1.1. Related Works

1.1.1. Studies on Pinching-Antenna Systems

Research on pinching-antenna systems has garnered growing interest, and current studies on pinching-antenna systems are diverse and consider various performance metrics. In [9], the downlink rate of a pinching-antenna system with a single user and multiple pinching antennas along a single waveguide was maximized. To proceed with the maximization, an approximately equivalent relaxed optimization problem was tackled in two stages. The position of the pinching antennas was determined to mitigate large-scale fading in the first stage, after which the position of the pinching antennas was tuned for constructive combining at the user. In [10], the minimum uplink rate of a multi-user pinching-antenna system with multiple pinching antennas and a single waveguide was maximized by optimizing the position of the pinching antennas and OMA resource allocation. In [11], the pinching-antenna system array gain with multiple pinching antennas along a waveguide was analyzed, where an upper bound of the array gain and the optimal number of pinching antennas were derived. A physics-based model for a pinching-antenna system was proposed in [12], and the transmit power was minimized with respect to the transmit beamforming and the position of pinching antennas. Both arbitrary and discrete (pre-configured) positions of the pinching antennas were considered in the optimization problem. In [13], a pinching-antenna system was employed in integrated sensing and communication (ISAC) systems, where the data rate was maximized while satisfying the sensing requirement. A two-waveguide pinching-antenna system-assisted ISAC design was proposed in [14], where the illumination power was maximized subject to communication quality of service (QoS) constraint.

1.1.2. Studies on NOMA-Assisted Pinching-Antenna Systems

Current research on NOMA-assisted pinching-antenna systems is also diverse, but several notable studies have focused on rate and efficiency metrics. In [15], by choosing which pinching antennas to activate, the downlink NOMA sum rate of a pinching-antenna system with fixed pinching antennas along a single waveguide was maximized. To simplify the problem, a matching algorithm was proposed. A low-complexity scheme for single and multiple pinching-antenna placement in time-division multiple access (TDMA) and single pinching-antenna placement in NOMA was proposed in [16]. In [17], the energy efficiency was maximized in an uplink NOMA-assisted pinching-antenna system, subject to the user transmit power and the position of the pinching antenna. In a cognitive radio-inspired NOMA (CR-NOMA) setting, Ref. [18] maximized the strong user data rate with respect to the power allocation and the position of the pinching antenna, subject to QoS requirements.

Alternating optimization was used in [19] to maximize the downlink sum rate of a NOMA-assisted pinching-antenna system with respect to the power allocation and the position of the pinching antennas.

1.2. Motivation and Contributions

6G is envisioned to tremendously improve the usage scenarios of 5G, and also to support new capabilities in areas such as sensing and artificial intelligence [8]. To meet this requirement, various key-enabling techniques such as flexible antennas and next-generation multiple access schemes can be incorporated into 6G. To further enhance the performance of the next-generation wireless network, we can tap into the synergies of these key-enabling techniques. A promising and interesting study is integrating NOMA in pinching-antenna systems. The ability of flexible antenna systems to reconfigure the wireless environment is a desirable feature in NOMA as it manages non-orthogonality through power disparities. For instance, as with reconfigurable intelligent surfaces (RISs) [20], by manipulating each user channel, flexible antenna systems can also enable QoS-based NOMA and dictate an SIC decoding order to satisfy the QoS requirement. On the other hand, NOMA is appealing for implementation in pinching-antenna systems as even though multiple pinching antennas are deployed to support multiple users, they can only transmit a single signal if they are along a single waveguide. Multiple users can be served by sending the superimposed signal and implementing SIC at the user [4].

In this article, we investigate the reliability of NOMA-assisted pinching-antenna systems. The growing interest in NOMA-assisted pinching-antenna system research has mainly focused on data rate and other efficiency metrics, and we aim to contribute to the body of research by analyzing another important metric, which is error rate. Recently, Ref. [21] analyzed and optimized the bit error rate (BER) performance of an uplink NOMA-assisted pinching-antenna system, and also performed some preliminary investigations on the downlink counterpart. However, the NOMA power allocation and the position of the pinching antenna are still coupled in the downlink optimization, which is also done numerically on a relatively complex BER expression. In this paper, by adopting the simplified SIC analysis in [22], where errors in imperfect SIC only happen to adjacent symbols, we are able to provide concise but accurate symbol error rate (SER) expressions, simplifying the SER minimization process and providing more useful insights and practical implementations. The contributions of this paper are summarized as follows:

- We analyze the QAM SER of a simplified downlink NOMA-assisted pinching-antenna system and derive the optimal power allocation and position of the pinching antenna for minimum SER in the high signal-to-noise ratio (SNR) region. In the high SNR region and with negligible waveguide attenuation, the NOMA power allocation and the position of the pinching antenna can be effectively decoupled and the optimization also reduced to numerically solving a rational function.
- We demonstrate that at practical higher-order QAM, the minimum SER strategy is for the pinching antenna to track the strong NOMA user.
- We simulate and verify the results with Monte Carlo simulation. We also simulate different practical NOMA-assisted pinching-antenna system scenarios.

To facilitate the analysis, we use SER instead of BER for the M-QAM error rate. Nevertheless, in the high SNR region and with gray coding, BER $\approx$ SER/$\log_2 M$.

This paper is organized as follows: Section 2 introduces the NOMA-assisted pinching-antenna system model. Section 3 presents the minimum SER analysis and design. Section 4 verifies the theoretical results via Monte Carlo simulation, and finally Section 5 concludes this paper.

https://doi.org/10.3390/telecom7050127

2. System Model

As illustrated in Figure 1 on three-dimensional coordinates, we consider a simplified downlink system with a NOMA pair communicating to the base station (BS) via a dielectric waveguide with a single pinching antenna. The number of users was limited in the simplified model to reduce the latency associated with SIC [23], and multiple users can be served by using a hybrid multiple access system, where each NOMA group can be allocated orthogonal resources such as in TDMA [24]. We denote the NOMA user with the stronger and weaker channel as the strong user and weak user, respectively. The waveguide is parallel to the x-axis and is elevated with height d, and the position of the pinching antenna is then denoted as $\psi_{\text{Pin}} = (x,0,d)$, while the users' positions are denoted as $\psi_m = (x_m,y_m,0)$, $m = 1,2$. As the position of the pinching antenna can be adjusted to a certain extent, we assume that the LoS path is available, and the non-line-of-sight (NLoS) components of the user channels are assumed to be negligible compared to the LoS components [4]. Hence, the user channel to the pinching antenna is modeled as

$$h_m^{\text{Pin}} = \frac{\eta^{\frac{1}{2}} e^{-j\frac{2\pi}{\lambda}|\psi_m - \psi_{\text{Pin}}|}}{|\psi_m - \psi_{\text{Pin}}|}, m = 1,2, \tag{1}$$

where $\eta = \frac{c^2}{16\pi^2 f_c^2}$, $\lambda = \frac{c}{f_c}$, c is the speed of light and f_c is the carrier frequency [4]. While the signal is also attenuated along the waveguide, the propagation loss is much smaller compared to that in free space. We then assume that the propagation loss of the waveguide is negligible so that the total propagation loss only depends on the distance between the pinching antenna and the users, simplifying the analysis. At the same time, such an assumption can also serve as an upper-bound performance of the system. Hence, we model the BS-user channel as $h_m = h_m^{\text{Pin}} e^{j\phi}$, where $\phi = \frac{2\pi}{\lambda/\eta_{\text{eff}}} d_{\text{BS-PA}}$ accounts for the phase shift along the waveguide, η_{eff} is the effective refractive index of the waveguide, and $d_{\text{BS-PA}}$ is the distance between the BS and the pinching antenna [4]. To facilitate the analysis, we assume that the channel state information (CSI) is known at all the nodes. The dynamic movement of the pinching antenna can introduce additional channel estimation overhead and errors. Several channel estimation techniques for pinching-antenna systems, such as those employing deep learning [25,26], can be utilized to handle the channel spatio-temporal variations with reduced pilot overheads. We also first assume that $|h_2| > |h_1|$, which we later validate when we define the feasible range of x. To facilitate such assumption, we constrain the strong user to be always nearer the waveguide (i.e., $|y_2| < |y_1|$), and without loss of generality, we also take $x_2 > x_1$. We denote $s_2 \in S_2$ and $s_1 \in S_1$ as the strong user M_2-QAM and weak user M_1-QAM symbols, respectively, where S_2 and S_1 are the corresponding QAM alphabets and $\mathrm{E}[|s_2|^2] = \mathrm{E}[|s_1|^2] = 1$. The BS transmits the superimposed signal $s_\Sigma = \sqrt{P_b}(\sqrt{a_1}s_1 + \sqrt{a_2}s_2)$, where P_b is the BS transmit power and a_1 and a_2, such that $a_1 > a_2$ and $a_1 + a_2 = 1$, are the power allocation factors. Hence, the received signals by the weak and strong users are given as

$$y_m = h_m s_\Sigma + n_m, m = 1,2, \tag{2}$$

where $n_m \sim \mathcal{CN}(0,\sigma_n^2)$ are complex Gaussian noises of variance σ_n^2, and we define $\rho = P_b/\sigma_n^2$ as the transmit SNR.

https://doi.org/10.3390/telecom7050127

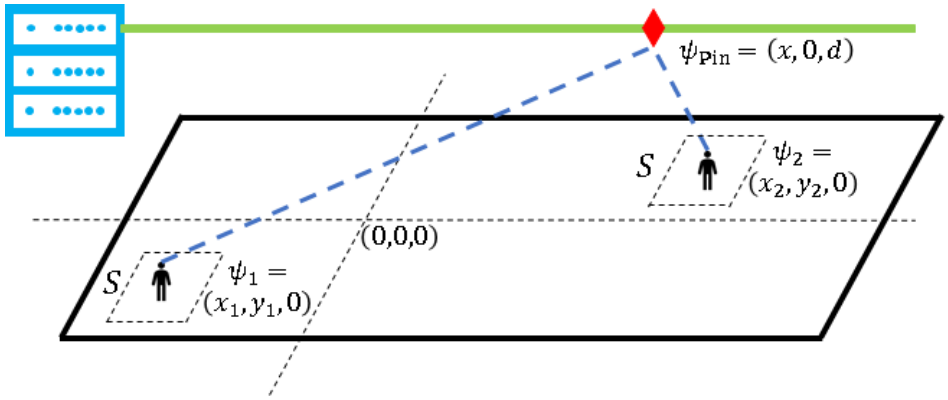


Figure 1. The system model of the NOMA-assisted pinching-antenna system network.

3. Minimum SER Design and Analysis

In this section, we discuss how the NOMA users can be tracked by the pinching antenna along the waveguide to minimize the SER. The weak user recovers s_1 as $\hat{s}_1 = \arg\min_{s_1 \in S_1} |y_1 - h_1\sqrt{P_b a_1} s_1|^2$ using Maximum Likelihood (ML) by treating s_2 as noise. The weak user SER $P_1(e)$ is computed by considering all (s_1,s_2) combinations and is given as

$$P_1(e) = \sum_{s_1 \in S_1} \sum_{s_2 \in S_2} P\{s_1\} P\{s_2\} P\{\hat{s}_1 \neq s_1 \mid s_1, s_2\}, \tag{3}$$

where $P\{E_A\}$ denotes the probability of event E_A and $P\{E_A|\, E_B\}$ denotes the probability of event E_A conditioned on event E_B. In the case of M-QAM symbols, the in-phase $s_{1,I}$ and quadrature $s_{1,Q}$ components of $s_1 = s_{1,I} + j s_{1,Q}$ are independently analyzed as $\sqrt{M}$-PAM symbols. A QAM symbol error occurs when either $\hat{s}_{1,I} \neq s_{1,I}$ or $\hat{s}_{1,Q} \neq s_{1,Q}$, and after simplifying,

$$P_1(e) = \frac{4(M_1 - \sqrt{M_1})}{M_1} \left(\frac{1}{\sqrt{M_2}} \sum_{n=-\sqrt{M_2}/2}^{\sqrt{M_2}/2-1} Q_{1,n} \right) - \frac{4(\sqrt{M_1} - 1)^2}{M_1 M_2} \sum \sum_{n,m=-\sqrt{M_2}/2}^{\sqrt{M_2}/2-1} Q_{1,n} Q_{1,m}, \tag{4}$$

where $Q_{1,n} = Q\left(\sqrt{\rho \alpha_{1,n}} |h_1|\right)$, $\alpha_{1,n} = \left(\sqrt{a_1/2} d_{M_1} + (2n+1)\sqrt{a_2/2} d_{M_2}\right)^2$, $d_{M_1} = \sqrt{6/(M_1 - 1)}$, $d_{M_2} = \sqrt{6/(M_2 - 1)}$ and $Q(x)$ is the q-function [27].

By using the same method, the strong user first recovers s_1 as $\hat{s}_1^{\text{SIC}} = \arg\min_{s_1 \in S_1} |y_2 - h_2\sqrt{P_b a_1} s_1|^2$, where $\hat{s}_1^{\text{SIC}} \in S_1$, and eventually recovers s_2 as $\hat{s}_2 = \arg\min_{s_2 \in S_2} |y_2 - h_2\sqrt{P_b}\left(\sqrt{a_1}\hat{s}_1^{\text{SIC}} + \sqrt{a_2} s_2\right)|^2$ by using SIC and ML again. The strong user SER $P_2(e)$ is computed by considering all $\left(s_1, s_2, \hat{s}_1^{\text{SIC}}\right)$ combinations and is given as

$$P_2(e) = \sum_{s_1 \in S_1} \sum_{s_2 \in S_2} P\{s_1\} P\{s_2\} P\{\hat{s}_1^{\text{SIC}} \mid s_1, s_2\} P\{\hat{s}_2 \neq s_2 \mid s_1, s_2, \hat{s}_1^{\text{SIC}}\}. \tag{5}$$

The system SER $P_{\text{sys}}(e)$ is given as

$$P_{\text{sys}}(e) = \frac{1}{2}(P_1(e) + P_2(e)). \tag{6}$$

We seek to minimize $P_{\text{sys}}(e)$ by dynamically adjusting the power allocation and the position of the pinching antenna based on the current positions of the NOMA user pair.

To facilitate the minimization of $P_{\text{sys}}(e)$, we use the compact approximation for $P_2(e)$ given in [22] as

$$\begin{aligned} P_2(e) = & \frac{4\left(\sqrt{M_2}-1\right)}{\sqrt{M_2}} Q_{2,1} - \frac{4\left(\sqrt{M_1}-1\right)\left(\sqrt{M_2}-1\right)}{\sqrt{M_2 M_1}} Q_{2,2} + \frac{4\left(\sqrt{M_1}-1\right)}{\sqrt{M_2 M_1}} Q_{2,3} \\ & - \frac{4\left(\sqrt{M_1}+\sqrt{M_2}-\sqrt{M_2 M_1}-2\right)}{\sqrt{M_2 M_1}} Q_{2,4} - \frac{4\left(\sqrt{M_1}-1\right)}{\sqrt{M_2 M_1}} Q_{2,5} \\ & - \sum \sum_{i,j=1}^{5} C_{ij} Q_{2,i} Q_{2,j}, \end{aligned} \tag{7}$$

where $Q_{2,i} = Q\left(\sqrt{\rho \alpha_{2,i}} |h_2|\right)$, $\alpha_{2,1} = \left(\sqrt{a_2/2} d_{M2}\right)^2$, $\alpha_{2,2} = \left(\sqrt{2a_1} d_{M_1} - \sqrt{a_2/2} d_{M2}\right)^2$, $\alpha_{2,3} = \left(\sqrt{a_1/2} d_{M_1} - \left(\sqrt{M_2}-1\right)\sqrt{a_2/2} d_{M2}\right)^2$, $\alpha_{2,4} = \left(\sqrt{2a_1} d_{M_1} + \sqrt{a_2/2} d_{M2}\right)^2$, $\alpha_{2,5} = \left(\sqrt{a_1/2} d_{M_1} + \left(\sqrt{M_2}-1\right)\sqrt{a_2/2} d_{M2}\right)^2$ and C_{ij} (given in Table A1 of Appendix A) are functions of M_1 and M_2. SER $P_2(e)$ was derived by considering only the adjacent symbols during imperfect SIC instead of $\hat{s}_1^{\text{SIC}} \in S_1$, e.g., $\hat{s}_{1,I}^{\text{SIC}} \in \left\{s_{1,I}^{\text{left}}, s_{1,I}, s_{1,I}^{\text{right}}\right\}$, where $s_{1,I}^{\text{left}}$ and $s_{1,I}^{\text{right}}$ are the left and right in-phase components adjacent to $s_{1,I}$.

In the high SNR region, $P_1(e) \to \frac{4\left(\sqrt{M_1}-1\right)}{\sqrt{M_1 M_2}} Q_{1,-\sqrt{M_2}/2}$ and $P_2(e) \to \frac{4\left(\sqrt{M_2}-1\right)}{\sqrt{M_2}} Q_{2,1} + \frac{4\left(\sqrt{M_1}-1\right)}{\sqrt{M_2 M_1}} Q_{2,3}$, and as $Q_{1,-\sqrt{M_2}/2} > Q_{2,3}$ since $|h_2| > |h_1|$, $P_{\text{sys}}(e) \to \frac{2\left(\sqrt{M_1}-1\right)}{\sqrt{M_1 M_2}} Q_{1,-\sqrt{M_2}/2} + \frac{2\left(\sqrt{M_2}-1\right)}{\sqrt{M_2}} Q_{2,1}$. As $|h_m| = \frac{\eta^{1/2}}{|\psi_m - \psi_{\text{Pin}}|}$, in the high SNR region, $P_{\text{sys}}(e)$ can be expressed as

$$P_{\text{sys}}(e) \approx \frac{2\left(\sqrt{M_1}-1\right)}{\sqrt{M_1 M_2}} Q_{1,\rho\to\infty} + \frac{2\left(\sqrt{M_2}-1\right)}{\sqrt{M_2}} Q_{2,\rho\to\infty}, \tag{8}$$

where $Q_{1,\rho\to\infty} = Q\left(\frac{\sqrt{\eta\rho}}{|\psi_1 - \psi_{\text{Pin}}|}\left(\sqrt{\frac{a_1}{2}} d_{M_1} - \left(\sqrt{M_2}-1\right)\sqrt{\frac{a_2}{2}} d_{M_2}\right)\right)$, $Q_{2,\rho\to\infty} = Q\left(\frac{\sqrt{\eta\rho}}{|\psi_2 - \psi_{\text{Pin}}|}\sqrt{\frac{a_2}{2}} d_{M2}\right)$, $|\psi_m - \psi_{\text{Pin}}| = \sqrt{(x - x_m)^2 + v_m^2}$, $v_m^2 = y_m^2 + d^2$ and $m = 1,2$. Our objective is to minimize $P_{\text{sys}}(e)$ in the high SNR region by finding the optimal power allocation and position of pinching antenna:

$$a_2^{\text{opt}}, x^{\text{opt}} = \arg\min_{a_2, x} P_{\text{sys}}(e), \tag{9}$$

where $a_2 \in (0, a_2^{\max})$ and $a_2^{\max} = \frac{M_2 - 1}{M_2 - 1 + \left(\sqrt{M_2}-1\right)^2 (M_1 - 1)}$ [27].

Proposition 1. *The optimal position of the pinching antenna x^{opt} along the waveguide minimizes $f(x)$ given as*

$$f(x) = f_1(x) + \left(f_2(x) + f_3(x)\right)^2, \tag{10}$$

where

$$f_1(x) = (M_2 - 1)\left((x - x_2)^2 + v_2^2\right) \tag{11a}$$

$$f_2(x) = \sqrt{M_1 - 1}\left(\sqrt{M_2} - 1\right)\sqrt{(x - x_2)^2 + v_2^2} \tag{11b}$$

$$f_3(x) = \sqrt{M_1 - 1}\sqrt{(x - x_1)^2 + v_1^2}. \tag{11c}$$

Proof of Proposition 1. As $Q_{1,\rho\to\infty}$ and $Q_{2,\rho\to\infty}$ is monotonically increasing and decreasing with increasing a_2, respectively, the minimum $P_{\text{sys}}(e)$ for a given ψ_{Pin} is achieved when

$Q_{1,\rho\to\infty} = Q_{2,\rho\to\infty}$ (please refer to Appendix B) and the optimal power allocation for a given channel strength ratio $R^{1/2} = \frac{|h_1|}{|h_2|} = \frac{|\psi_2-\psi_{\text{Pin}}|}{|\psi_1-\psi_{\text{Pin}}|}$ is given in [28] as

$$a_2^{\text{opt}} = \frac{M_2 - 1}{M_2 - 1 + \left(\sqrt{M_2} - 1 + R^{-1/2}\right)^2 (M_1 - 1)} < a_2^{\max}. \tag{12}$$

At a_2^{opt} for a given $\psi_{\text{Pin}} = (x,0,d)$, we denote $Q_e(x) = Q_{1,\rho\to\infty} = Q_{2,\rho\to\infty}$ and $P_{\text{sys}}(e) \approx 2\left(1 - \frac{1}{\sqrt{M_2 M_1}}\right) Q_e(x)$. Using $Q_{2,\rho\to\infty}$, $Q_e(x)$ can be expressed as $Q_e(x) = Q\left(\frac{\sqrt{\eta\rho}}{|\psi_2-\psi_{\text{Pin}}|}\sqrt{\frac{a_2^{\text{opt}}}{2}} d_{M2}\right)$ and after some simplification, $Q_e(x)$ can be expressed as $Q_e\left(\frac{3\eta}{f(x)}\right)$, where $f(x)$ is given in (10), and minimizing $f(x)$ leads to a minimum $P_{\text{sys}}(e)$.

As $f_1(x), f_2(x)$ and $f_3(x)$ are all positive convex functions, it follows that $f_{2+3}(x) = f_2(x) + f_3(x)$, $f_{2+3}^2(x)$ and finally $f(x)$ are also convex. The first and second derivatives of $f(x)$ are also given as

$$\frac{df(x)}{dx} = 2\sqrt{M_1 - 1}(f_2(x) + f_3(x)) f_4(x) + 2(M_2 - 1)(x - x_2) \tag{13a}$$

$$\frac{d^2 f(x)}{dx^2} = 2(M_2 - 1) + 2\Big((M_1 - 1) f_4^2(x) + (f_2(x) + f_3(x)) f_5(x)\Big), \tag{13b}$$

where

$$f_4(x) = \frac{(x - x_1)}{\sqrt{(x - x_1)^2 + v_1^2}} + \frac{\left(\sqrt{M_2} - 1\right)(x - x_2)}{\sqrt{(x - x_2)^2 + v_2^2}} \tag{14a}$$

$$f_5(x) = \sqrt{M_1 - 1}\left(\frac{v_1^2}{\sqrt{((x - x_1)^2 + v_1^2)^3}} + \frac{\left(\sqrt{M_2} - 1\right) v_2^2}{\sqrt{((x - x_2)^2 + v_2^2)^3}}\right). \tag{14b}$$

As $f_5(x) > 0$, $\frac{d^2 f(x)}{dx^2} > 0, f(x)$ is strictly convex and x^{opt} is unique. To find x^{opt}, we can solve $\frac{df(x)}{dx} = 0$. □

Unfortunately, it is not straightforward to analytically solve $\frac{df(x)}{dx} = 0$. To facilitate solving for x numerically, we limit $x \in (x_{\min}, x_{\max}]$.

Proposition 2. *The feasible region for x is* $x \in (x_{\min}, x_{\max}]$, *where* $x_{min} = \frac{1}{2}\left(\frac{\|\psi_1\|^2 - \|\psi_2\|^2}{x_1 - x_2}\right)$ *and* $x_{max} = x_2$.

Proof of Proposition 2. The minimum x can be obtained from the NOMA principle of $|h_2| > |h_1|$, which translates to $|\psi_2 - \psi_{\text{Pin}}| < |\psi_1 - \psi_{\text{Pin}}|$ or, from Figure 1 (users along the xy-plane with $x_2 > x_1$), $x > x_{\min}$, where $x_{\min} = \frac{1}{2}\left(\frac{\|\psi_1\|^2 - \|\psi_2\|^2}{x_1 - x_2}\right)$.

We note that for any $\delta > 0$, $|h_2(x_2 + \delta)| = |h_2(x_2 - \delta)|$ but $|h_1(x_2 - \delta)| \geq |h_1(x_2 + \delta)|$ since $|\psi_1(x_2 - \delta) - \psi_{\text{Pin}}| < |\psi_1(x_2 + \delta) - \psi_{\text{Pin}}|$. Hence, using (8), $P_{\text{sys}}(e, x_2 + \delta) \geq \hat{P}_{\text{sys}}(e, x_2 - \delta) \geq P_{\text{sys}}(e, x_2 - \delta)$, where $P_{\text{sys}}(e,x_2 + \delta)$ and $P_{\text{sys}}(e,x_2 - \delta)$ is the system error for $x = x_2 + \delta$ and $x = x_2 - \delta$, respectively, and $\hat{P}_{\text{sys}}(e, x_2 - \delta)$ is the system error for $x = x_2 - \delta$ and computed optimal power allocation for $x = x_2 + \delta$. As $P_{\text{sys}}(e,x_2 + \delta) \geq P_{\text{sys}}(e,x_2 - \delta)$, we limit $x_{\max} = x_2$. □

Numerically solving $\frac{df(x)}{dx} = 0$ to obtain x^{opt}, in the high SNR region and for stationary users, $P_{\text{sys}}(e)$ is given as

$$P_{\text{sys}}^{\text{opt}}(e) \approx 2\left(1 - \frac{1}{\sqrt{M_2 M_1}}\right) Q_e\left(x^{\text{opt}}\right). \tag{15}$$

If we take into account the waveguide attenuation, we can express the overall channel attenuation as $|h_m(x)| = |P_L(x)||h_m^{\text{Pin}}(x)|$, where $|P_L(x)| = 10^{-\frac{\kappa}{20}|x-x_{\text{BS}}|}$, κ is the attenuation factor along the waveguide and $|x - x_{\text{BS}}|$ is the distance between the pinching antenna and the BS situated at $y = 0$. The optimal power allocation (12) for the users still holds, so the power allocation and the position of the pinching antenna can still be decoupled during the optimization process. However, $Q_{1,\rho\to\infty} \approx Q_{2,\rho\to\infty}$ does not strictly hold, so x^{opt} must be solved by minimizing the $P_{\text{sys}}(e)$ given in (6). As $\rho \to \infty$, $C_{ij}Q_{2,i}Q_{2,j}$ components of $P_2(e)$ may be ignored during optimization, so $P_{\text{sys}}(e)$ will just comprise several $K_iQ(g_i(x))$ terms, and numerical minimization to find x^{opt} may be applied afterwards.

Proposition 3. *For strong user higher-order modulations, $x_2 \approx x^{opt}$ and x_2 is near-optimal.*

Proof of Proposition 3. $\frac{1}{(M_1-1)\left(\sqrt{M_2}-1\right)^2}\frac{df(x)}{dx}$ can be expressed as

$$\begin{aligned}\frac{df(x)/dx}{(M_1-1)\left(\sqrt{M_2}-1\right)^2} &= (x-x_1)\left(\frac{2}{\sqrt{M_2}-1}\frac{\sqrt{(x-x_2)^2+v_2^2}}{\sqrt{(x-x_1)^2+v_1^2}}+\frac{2}{\left(\sqrt{M_2}-1\right)^2}\right)\\ &+(x-x_2)\left(2+\frac{2}{\sqrt{M_2}-1}\frac{\sqrt{(x-x_1)^2+v_1^2}}{\sqrt{(x-x_2)^2+v_2^2}}+\frac{2}{M_1-1}\frac{M_2-1}{\left(\sqrt{M_2}-1\right)^2}\right).\end{aligned} \tag{16}$$

For high orders of M_2, we assume that $\frac{1}{\sqrt{M_2}-1} \approx 0$, $\frac{M_2-1}{\left(\sqrt{M_2}-1\right)^2} \approx 1$, and $\frac{1}{(M_1-1)\left(\sqrt{M_2}-1\right)^2}\frac{df(x)}{dx} \approx \left(2+\frac{2}{M_1-1}\right)(x-x_2)$. Hence, $\frac{df(x)}{dx} \approx 0$ at $x^{\text{opt}} \approx x_2$, or tracking the strong user is near optimal at large M_2. □

Hence, the minimum SER strategy at higher-order modulations is for the pinching antenna to track the strong user, and to use the SER-optimal NOMA power factor in (12). The system SER approaches

$$\overset{\sim\text{opt}}{P}_{\text{sys}}(e) \approx 2Q_e(x_2), \tag{17}$$

where $\overset{\sim\text{opt}}{P}_{\text{sys}}(e)$ is $P_{\text{sys}}^{\text{opt}}(e)$ at higher-order modulation.

Due to the possible speed limitation of the pinching antenna, it may not be possible to completely track the strong user. An alternative tracking implementation is to use multiple stationary pinching antennas, with only the pinching antenna nearest to the strong user activated. Compared to stationary pinching antennas, mobile pinching antennas may also compound the Doppler effect for some mobile users (e.g., moving in opposite directions) if the antenna movement is not slow.

4. Simulation

In this section, we verify our analysis using computer simulation. Following [29], we set f_c = 28 GHz, d = 3 m, $\sigma_n^2 = -90$ dBm and the BS transmit power budget at 40 dBm. To simulate the waveguide attenuation, we set the waveguide attenuation factor as κ = 0.1 dB/m [21]. The position of the users is uniformly randomly distributed on squares along the xy-plane with side S = 2. The location of the weak and strong users is centered around (−4,−4,0) and (22,2,0), respectively, satisfying $|y_2| < |y_1|$, while the BS is situated at (x,y) = (−6,0). In such a scenario, NOMA is more justifiable to apply, since the strong and weak user channel can be made more disparate, depending on the position of the pinching antenna in the waveguide. The simulated SERs were obtained by averaging over

10^8 symbol pairs for each $(M_1,M_2) \in \{(4,4),(4,16),(16,16)\}$. MATLAB was used for the Monte Carlo simulation and the *vpasolve* function was used to solve for x^{opt} in $\frac{df(x)}{dx} = 0$.

The SER performance of the NOMA-assisted pinching-antenna system with optimal power allocation and stationary pinching antenna at $x = x^{\text{opt}}$ for stationary users at the center of their squares is shown in Figure 2. The simulation data matches the theoretical equations and is close to the high SNR approximation. The SER performance of power-only optimization with $x = 1.2x^{\text{opt}}$ and $x = 0.8x^{\text{opt}}$ were also simulated as baselines to illustrate the optimality of $x = x^{\text{opt}}$, which becomes more evident as the modulation orders increase. Also simulated was $x = x_2$, where the pinching antenna is nearest to the strong user. It can be seen that the performance of $x = x_2$ approaches that of $x = x^{\text{opt}}$ as M_2 increases. For instance, at $(M_1,M_2) = (16,16)$, $x^{\text{opt}} = 20.7997$, which is close to $x_2 = 22$. At the next modulation order of $(M_1,M_2) = (64,64)$, x^{opt} is computed to be closer to x_2 at $x^{\text{opt}} = 21.4947$, consistent with Proposition 3. The current-generation wireless system 5G can support until 1024-QAM [30] and, for example, when $(M_1,M_2) = (16,256)$, where $\frac{1}{\sqrt{M_2}-1} = 0.0667$ and $\frac{M_2-1}{\left(\sqrt{M_2}-1\right)^2} = 1.1333$, or the order of magnitude of error is -1 for the assumptions $\frac{1}{\sqrt{M_2}-1} \approx 0$ and $\frac{M_2-1}{\left(\sqrt{M_2}-1\right)^2} \approx 1$, x^{opt} is much closer to x_2 at $x^{\text{opt}} = 21.7750$. Taking into account the waveguide attenuation, from the simulation it can be seen that there is roughly 2 to 3 dBm loss to achieve the same SER performance ($x = x^{\text{opt}}$,WG). At $x^{\text{opt}} = 20.7997$ for $(M_1,M_2) = (16,16)$, $|P_L(x)| = 0.7345$, while $\left|h_2^{\text{Pin}}(x)\right| = 2.2437 \times 10^{-4}$, showing that on the system model, most of the attenuation is due to the free-space channel. Localization errors that would result in imperfect CSI were also simulated ($x = x^{\text{opt}}$,ICSI) by slightly changing the users' estimated position ($\psi'_m = 0.99\psi_m$). Performance loss on CSI errors seems more pronounced on higher-order modulations, where there is less inter-symbol spacing.

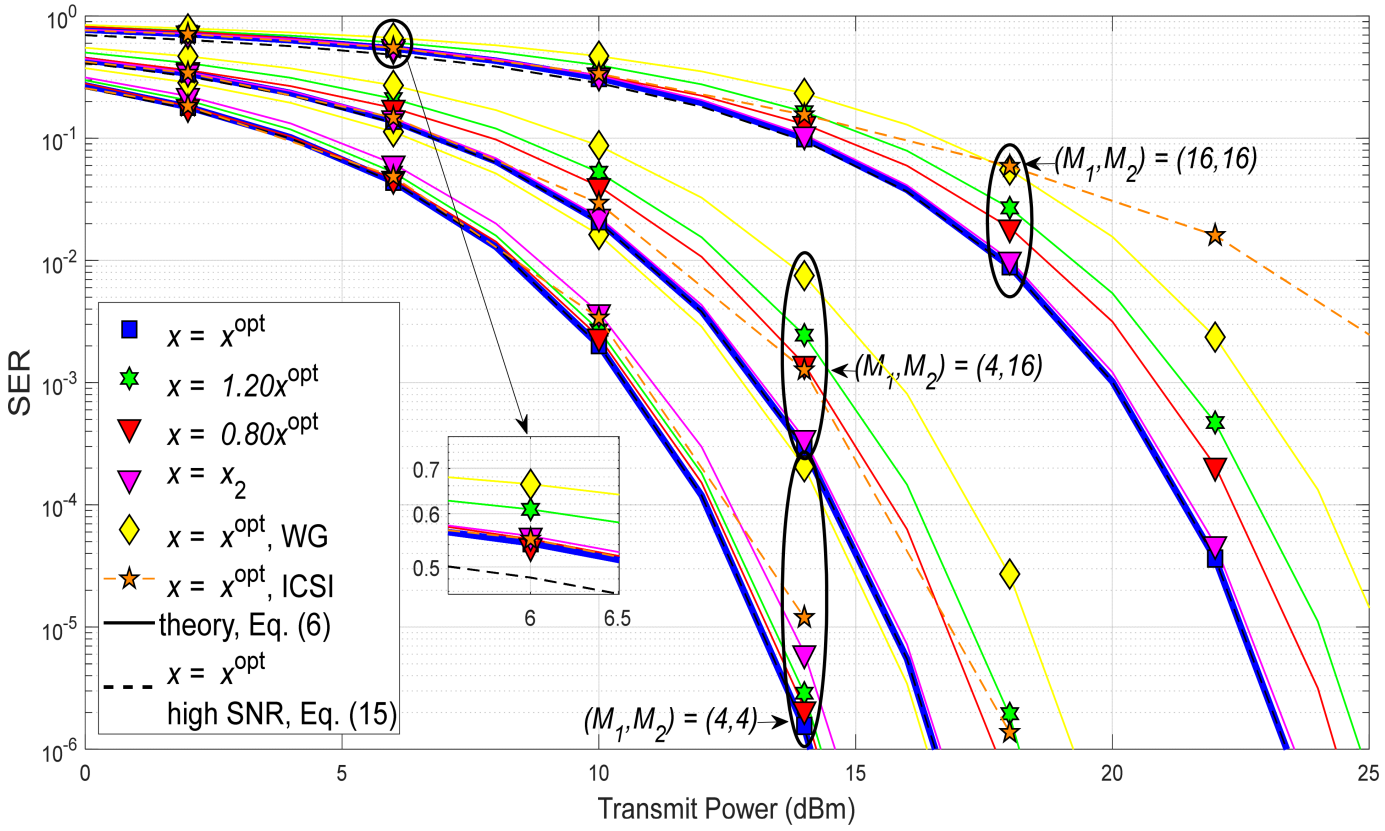


Figure 2. SER performance of NOMA-assisted stationary pinching-antenna system.

The SER performance of the non-stationary pinching antenna and users is likewise simulated in Figure 3. The performance of the stationary and non-stationary NOMA-assisted pinching-antenna system are similar. If the users are confined to be randomly situated within a larger area, multiple fixed pinching antennas (activated one at a time) at discrete points may be a good alternative to a single, mobile one, as stationary antennas may be less susceptible to channel estimation errors, and less energy may be consumed by avoiding mechanical movement. In the system model, the user distribution is simplified by assuming that the users are spatially uniformly distributed within a confined space, and that the pinching antenna can track the users instantaneously. The average SER $\overline{P_{\text{sys}}}(e)$, where $\overline{P_{\text{sys}}}(e) = \mathrm{E}\left[P_{\text{sys}}(e)\right]$ is averaged over the distribution of x^{opt}, is difficult to compute since it is difficult to derive the closed-form expression of x^{opt}, and the distribution of x^{opt} also depends on the distribution of location of the strong and weak users.

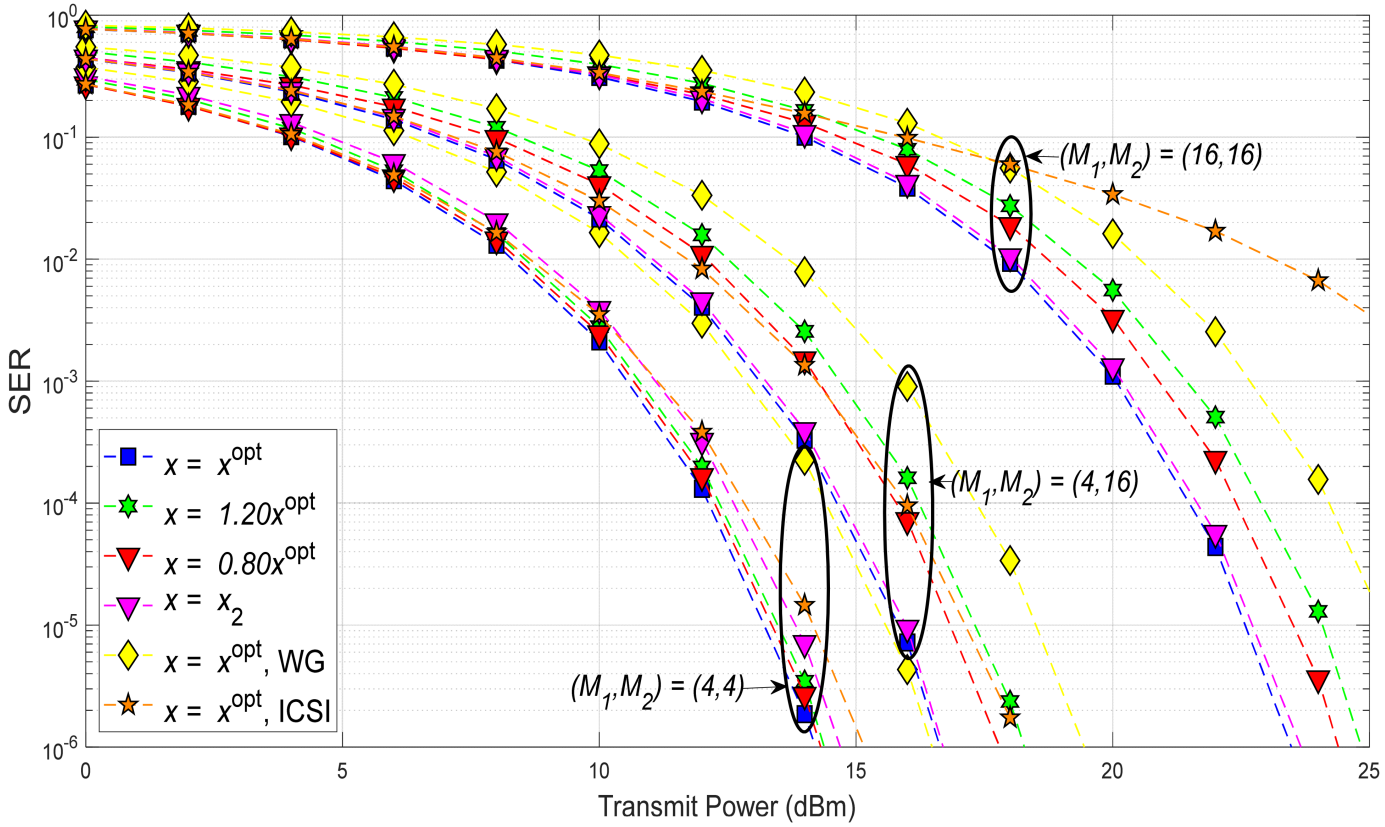


Figure 3. SER performance of NOMA-assisted non-stationary pinching-antenna system.

The SER performance of the NOMA-assisted pinching-antenna system with different configurations is simulated in Figure 4. The SER performance of optimal power allocation, mobile users and stationary pinching antenna on $x = x^{\text{opt}}$ for stationary users at the center of their squares is almost the same with that of the mobile pinching antenna. To reduce the complexity, fixed power allocation, which is optimal when $x = x^{\text{opt}}$ for stationary users at the center of their squares, is also simulated. There is a noticeable performance loss when the power allocation does not adapt to the users' location. Finally, random positioning of the pinching antenna with optimal power allocation is also simulated, and it can be seen that it has a bad SER performance, indicating that sensible pinching-antenna positioning is important.

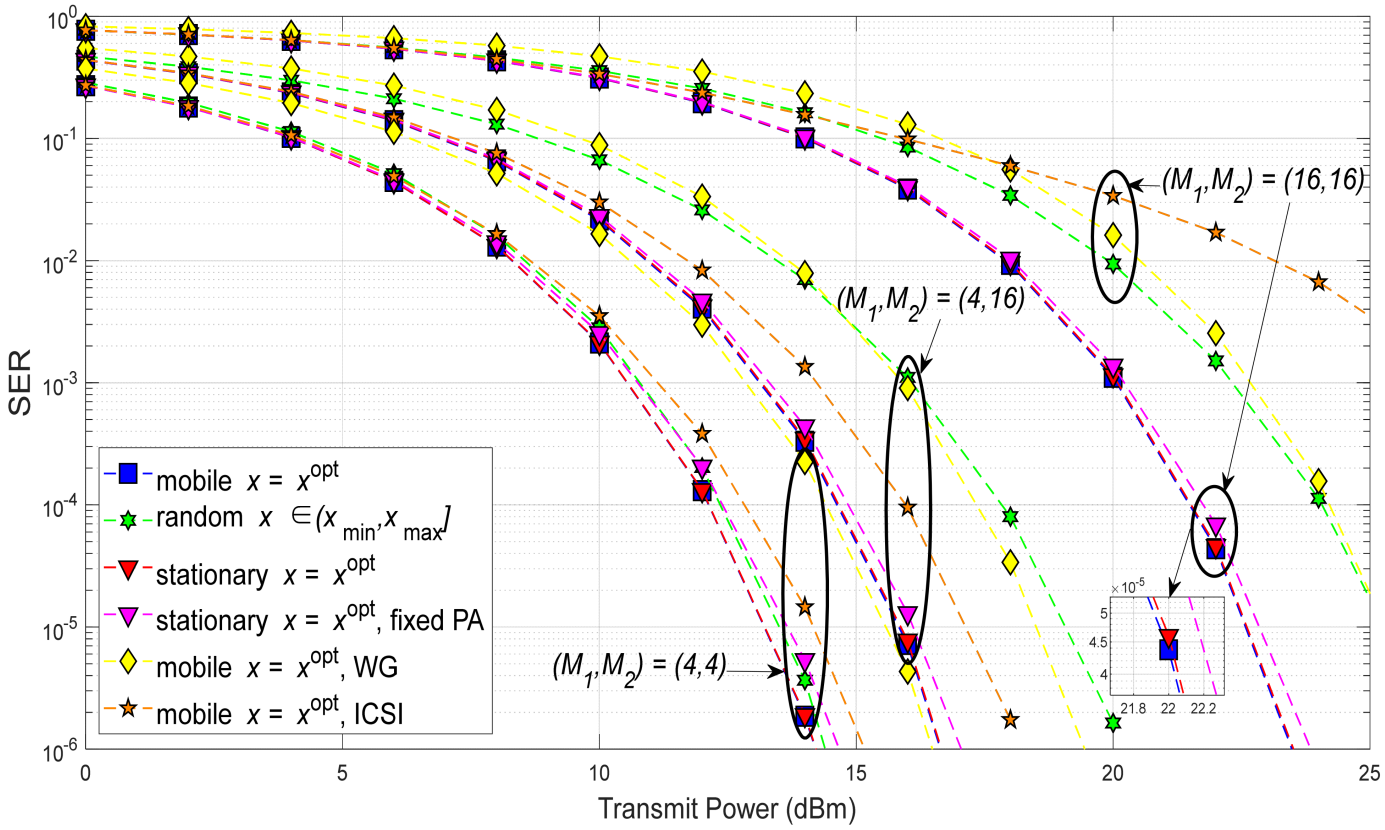


Figure 4. SER performance of NOMA-assisted pinching-antenna system with different configurations.

5. Conclusions

In this article, we analyzed the downlink NOMA-assisted pinching-antenna system SER performance. The minimum SER expression in the high SNR region was derived and a procedure to obtain the optimal position of the pinching antenna and the corresponding power allocation was presented. At higher-order modulation for the strong user, it was also revealed that the minimum NOMA SER strategy is for the pinching antenna to track the strong user, and assign SER-optimal power allocation to the NOMA users. The analysis was verified via MATLAB simulation. To facilitate the analysis, a very idealized system model was adopted and many practical simplifications such as the minimal number of users and antenna, perfect CSI, and instantaneous user tracking of the pinching antenna were assumed. Research that takes into account practical considerations is important for real-world deployment. Hence, future work can include multiple users utilizing hybrid OMA-NOMA schemes, multiple pinching antennas, imperfect CSI due to localization with limited accuracy, and mobile pinching antennas with limited speed. The optimal position of the pinching antenna was also derived numerically, and to quantify the system SER for mobile users, another possible future research direction is to derive a closed-form expression or accurate approximation of x^{opt}.

Funding: This research received no external funding.

Data Availability Statement: The original contributions presented in this study are included in the article. Further inquiries can be directed to the corresponding author.

Conflicts of Interest: The author declares no conflicts of interest.

Appendix A. C_{ij} Values

Table A1. C_{ij} values for (7).

C_{ij}	Values
C_{11}	$-\frac{4\left(M_2-2\sqrt{M_2}+1\right)}{M_2}$
C_{12}	$\frac{8\left(\sqrt{M_1}-1\right)\left(M_2-2\sqrt{M_2}\right)}{M_2\sqrt{M_1}}$
C_{13}	$-\frac{8\left(2\left(\sqrt{M_1}-1\right)\left(\sqrt{M_2}-2\right)+\left(\sqrt{M_1}-1\right)\left(M_2-4\sqrt{M_2}+4\right)+\sqrt{M_1}\right)}{M_2\sqrt{M_1}}$
C_{14}	$-\frac{8\left(\sqrt{M_1}-1\right)\left(\sqrt{M_2}-1\right)}{M_2\sqrt{M_1}}$
C_{15}	$\frac{8\left(\sqrt{M_1}-1\right)\left(\sqrt{M_2}-1\right)}{M_2\sqrt{M_1}}$
C_{22}	$-\frac{4\left(\sqrt{M_1}-1\right)^2\left(M_2-2\sqrt{M_2}+1\right)}{M_2M_1}$
C_{23}	$\frac{8\left(\sqrt{M_1}-1\right)\left(\sqrt{M_1}+\left(\sqrt{M_2}-2\right)\left(2\sqrt{M_1}-1\right)+\left(\sqrt{M_1}-1\right)\left(M_2-4\sqrt{M_2}+4\right)\right)}{M_2M_1}$
C_{24}	$\frac{8\left(\sqrt{M_1}-1\right)^2\left(\sqrt{M_2}-1\right)}{M_2M_1}$
C_{25}	$-\frac{8\left(\sqrt{M_1}-1\right)^2\left(\sqrt{M_2}-1\right)}{M_2M_1}$
C_{33}	$-\frac{4\left(\left(\sqrt{M_1}-1\right)^2\left(M_2-4\sqrt{M_2}+4\right)+2\left(\sqrt{M_1}-1\right)\left(\sqrt{M_2}-2\right)\sqrt{M_1}+M_1\right)}{M_2M_1}$
C_{34}	$-\frac{8\left(\sqrt{M_1}-1\right)\left(\sqrt{M_1}+\left(\sqrt{M_1}-1\right)\left(\sqrt{M_2}-2\right)\right)}{M_2M_1}$
C_{35}	$\frac{8\left(\sqrt{M_1}-1\right)\left(\sqrt{M_1}+\left(\sqrt{M_1}-1\right)\left(\sqrt{M_2}-2\right)\right)}{M_2M_1}$
C_{44}	$-\frac{4\left(\sqrt{M_1}-1\right)^2}{M_1M_2}$
C_{45}	$\frac{8\left(\sqrt{M_1}-1\right)^2}{M_1M_2}$
C_{55}	$-\frac{4\left(\sqrt{M_1}-1\right)^2}{M_1M_2}$

Appendix B. Proof of $P_{\mathrm{sys}}(e) \to \frac{2(\sqrt{M_1}-1)}{\sqrt{M_1M_2}}Q_{1,-\sqrt{M_2}/2} + \frac{2\left(\sqrt{M_2}-1\right)}{\sqrt{M_2}}Q_{2,1}$

Proof. When $a_2 \in (0, a_2^{\max})$, $P_{\mathrm{sys}}(e)$ can be expressed in the form $P_{\mathrm{sys}}(e) \approx A_1Q_{1,\delta}(\beta+\delta) + A_2Q_{2,\delta}(\beta - M\delta)$, where $M > 0$, δ can take the values of $\delta = 0$, $-\beta < \delta < 0$, or $\delta > 0$ (implying $M < \beta/\delta$). When $\delta = 0$, $Q_{1,\delta}(\beta) = Q_{2,\delta}(\beta) = Q(\beta)$. A pair of bounds for $Q(z)$, which is asymptotically tight as $z \to \infty$, is given by $\frac{z}{1+z^2}\phi(z) < Q(z) < \frac{1}{z}\phi(z)$, where $\phi(z) = \frac{1}{\sqrt{2\pi}}e^{-z^2/2}$ [31].

We analyze the asymptotic behavior using the upper bound, as a similar procedure also applies when using the lower bound. As $Q(z) \to \frac{1}{z}\phi(z)$, when $z \to \infty$, the asymptotic $P_{\mathrm{sys}}(e)$ can be expressed as $P_{\mathrm{sys}}^{\mathrm{UB}}(e) \approx \frac{1}{\sqrt{2\pi\rho}}e^{-\frac{\rho\beta^2}{2}}\left(A_1e^{-\frac{\rho e_1(\delta)}{2}-\ln(\beta+\delta)} + A_2e^{-\frac{\rho}{2}e_2(\delta)-\ln(\beta-M\delta)}\right)$, where $e_1(\delta) = \delta(2\beta+\delta)$ and $e_2(\delta) = M\delta(M\delta-2\beta)$. It can be verified that when $-\beta < \delta < 0$, $e_1(\delta) < 0$ and $c_1 = A_1e^{-\frac{\rho e_1(\delta)}{2}-\ln(\beta+\delta)}$ increases indefinitely as $\rho \to \infty$. Likewise, when $\delta > 0$, $e_2(\delta) < 0$ and $c_2 = A_2e^{-\frac{\rho}{2}e_2(\delta)-\ln(\beta-M\delta)}$ increases indefinitely as $\rho \to \infty$. At $\delta = 0$, $e_1(\delta) = e_2(\delta) = 0$, and $c_1 + c_2$ is asymptotically minimized. Hence, as $\rho \to \infty$, $P_{\mathrm{sys}}(e)$ is minimized when $Q_{1,\rho\to\infty} = Q_{2,\rho\to\infty}$. □

References

1. Yu, X.; Wang, J.; Hu, R.Q.; Kim, D.I.; Al-Dhahir, N.; Wymeersch, H.; Zhao, N. Intelligent flexible position antenna systems for networking: A survey. *IEEE Trans. Netw. Sci. Eng.* **2026**, *13*, 3105–3126. [CrossRef]
2. Zhu, L.; Ma, W.; Zhang, R. Modeling and performance analysis for movable antenna enabled wireless communications. *IEEE Trans. Wirel. Commun.* **2024**, *23*, 6234–6250. [CrossRef]
3. Wong, K.-K.; Tong, K.-F.; Zhang, Y.; Zhongbin, Z. Fluid antenna system for 6G: When bruce lee inspires wireless communications. *Electron. Lett.* **2020**, *56*, 1288–1290. [CrossRef]
4. Ding, Z.; Schober, R.; Poor, H.V. Flexible-antenna systems: A pinching-antenna perspective. *IEEE Trans. Commun.* **2025**, *73*, 9236–9253. [CrossRef]
5. Khammammetti, V.; Mohammed, S.K. OTFS-based multiple-access in high Doppler and delay spread wireless channels. *IEEE Wirel. Commun. Lett.* **2018**, *8*, 528–531. [CrossRef]
6. Shi, C.; Xie, Z.; Kang, P.; Cai, X.; Guo, L.; Fang, Y.; Chen, P. Enhanced pilot design for collision-resilient unsourced random access in massive MIMO. *IEEE Trans. Wirel. Commun.* **2026**, *25*, 17620–17633. [CrossRef]
7. Gui, G.; Liu, M.; Tang, F.; Kato, N.; Adachi, F. 6G: Opening new horizons for integration of comfort, security, and intelligence. *IEEE Wirel. Commun.* **2020**, *27*, 126–132. [CrossRef]
8. ITU-R, Draft New Recommendation. Framework and Overall Objectives of the Future Development of IMT for 2030 and Beyond. 2023. Available online: https://www.itu.int/dms_pubrec/itu-r/rec/m/R-REC-M.2160-0-202311-I!!PDF-E.pdf (accessed on 6 July 2026).
9. Xu, Y.; Ding, Z.; Karagiannidis, G.K. Rate maximization for downlink pinching-antenna systems. *IEEE Wirel. Commun. Lett.* **2025**, *14*, 1431–1435. [CrossRef]
10. Tegos, S.A.; Diamantoulakis, P.D.; Ding, Z.; Karagiannidis, G.K. Minimum data rate maximization for uplink pinching-antenna systems. *IEEE Wirel. Commun. Lett.* **2025**, *14*, 1516–1520. [CrossRef]
11. Ouyang, C.; Wang, Z.; Liu, Y.; Ding, Z. Array gain for pinching-antenna systems (PASS). *IEEE Commun. Lett.* **2025**, *29*, 1471–1475. [CrossRef]
12. Wang, Z.; Ouyang, C.; Mu, X.; Liu, Y.; Ding, Z. Modeling and beamforming optimization for pinching-antenna systems. *IEEE Trans. Commun.* **2025**, *73*, 13904–13919. [CrossRef]
13. Qin, Y.; Fu, Y.; Zhang, H. Joint antenna position and transmit power optimization for pinching antenna-assisted ISAC systems. *IEEE Wirel. Commun. Lett.* **2025**, *14*, 3535–3539. [CrossRef]
14. Zhang, Z.; Wang, Z.; Mu, X.; He, B.; Chen, J.; Liu, Y. Integrated sensing and communications for pinching-antenna systems (PASS). *IEEE Commun. Lett.* **2025**, *29*, 2929–2933. [CrossRef]
15. Wang, K.; Ding, Z.; Schober, R. Antenna activation for NOMA assisted pinching-antenna systems. *IEEE Wirel. Commun. Lett.* **2025**, *14*, 1526–1530. [CrossRef]
16. Xie, X.; Fang, F.; Ding, Z.; Wang, X. A low-complexity placement design of pinching-antenna systems. *IEEE Commun. Lett.* **2025**, *29*, 1784–1788. [CrossRef]
17. Zeng, M.; Li, X.; Wang, J.; Huang, G.; Dobre, O.A.; Ding, Z. Energy-efficient resource allocation for NOMA-assisted uplink pinching-antenna systems. *IEEE Wirel. Commun. Lett.* **2025**, *14*, 3695–3699. [CrossRef]
18. Xu, Y.; Ding, Z.; Cai, D.; Wong, V.W.S. QoS-aware NOMA design for downlink pinching-antenna systems. *IEEE Trans. Commun.* **2025**, *73*, 13611–13625. [CrossRef]
19. Zhou, Z.; Yang, Z.; Chen, G.; Ding, Z. Sum-rate maximization for NOMA-assisted pinching-antenna systems. *IEEE Wirel. Commun. Lett.* **2025**, *14*, 2728–2732. [CrossRef]
20. Liu, Y.; Mu, X.; Liu, X.; Di Renzo, M.; Ding, Z.; Schober, R. Reconfigurable intelligent surface-aided multi-user networks: Interplay between NOMA and RIS. *IEEE Wirel. Commun.* **2022**, *29*, 169–176. [CrossRef]
21. AlaaEldin, M.; Inwood, A.S.; Mu, X.; Matthaiou, M. BER analysis and optimization of pinching-antenna-based NOMA communications. *arXiv* **2026**. [CrossRef]
22. Rito, B.Y.D.; Li, K.H. RIS-assisted NOMA with interference-cancellation and interference-alignment scheme. *IEEE Commun. Lett.* **2023**, *27*, 1011–1015. [CrossRef]
23. Assaf, T.; Al-Dweik, A.; Moursi, M.S.E.; Zeineldin, H.; Al-Jarrah, M. NOMA receiver design for delay-sensitive systems. *IEEE Syst. J.* **2021**, *15*, 5606–5617. [CrossRef]
24. Ding, Z.; Fan, P.; Poor, H.V. Impact of user pairing on 5G nonorthogonal multiple access. *IEEE Trans. Veh. Technol.* **2016**, *65*, 6010–6023. [CrossRef]
25. Xiao, J.; Wang, J.; Liu, Y. Channel estimation for pinching-antenna systems (PASS). *IEEE Commun. Lett.* **2025**, *29*, 1789–1793. [CrossRef]
26. Lv, S.; Liu, T.; Yang, R.; Li, M.; Liu, Y. Deep learning-driven time-varying fading channel estimation for pinching antenna systems. *IEEE Wirel. Commun. Lett.* **2026**, *15*, 2569–2573. [CrossRef]

27. Lee, I.-H.; Kim, J.-B. Average symbol error rate analysis for non-orthogonal multiple access with M-Ary QAM signals in Rayleigh fading channels. *IEEE Commun. Lett.* **2019**, *23*, 1328–1331. [CrossRef]
28. Wang, Y.; Wang, J.; Ng, D.W.K.; Schober, R.; Gao, X. A minimum error probability NOMA design. *IEEE Trans. Wirel. Commun.* **2021**, *20*, 4221–4237. [CrossRef]
29. Li, Y.; Wang, J.; Liu, Y.; Ding, Z. Pinching-antenna assisted simultaneous wireless information and power transfer. *IEEE Commun. Lett.* **2025**, *29*, 2341–2345. [CrossRef]
30. Singya, P.K.; Shaik, P.; Kumar, N.; Bhatia, V.; Alouini, M.-S. A survey on higher-order QAM constellations: Technical challenges, recent advances, and future trends. *IEEE Open J. Commun. Soc.* **2021**, *2*, 617–655. [CrossRef]
31. Borjesson, P.; Sundberg, C.-E. Simple Approximations of the Error Function Q(x) for Communications Applications. *IEEE Trans. Commun.* **1979**, *27*, 639–643. [CrossRef]

Disclaimer/Publisher's Note: The statements, opinions and data contained in all publications are solely those of the individual author(s) and contributor(s) and not of MDPI and/or the editor(s). MDPI and/or the editor(s) disclaim responsibility for any injury to people or property resulting from any ideas, methods, instructions or products referred to in the content.